



Interdiffusion and Atomic Mobilities Studies in Ni-Rich fcc Ni-Ti-V Alloys

C. P. Wang¹ · W. H. Zhang¹ · X. Yu¹ · Z. B. Wei¹ · J. B. Zhang¹ · Y. Lu¹ · X. J. Liu^{1,2}

Submitted: 23 January 2023 / in revised form: 21 May 2023 / Accepted: 23 May 2023 / Published online: 21 June 2023
© ASM International 2023

Abstract The diffusion couples of Ni-Ti-V ternary alloys prepared and annealed at 1373 and 1473 K have been measured by electronic-probe microanalysis. Based on the concentration profiles, the interdiffusion coefficients were determined by using the Whittle and Green method. The atomic mobilities of the Ni-Ti-V ternary alloys were assessed based on the interdiffusion coefficients reported in the literature and the data obtained from the present work. In the comprehensive comparison, it was found that the model-predicted diffusion properties were in good agreement with the experimental data, which indicated that the diffusion phenomena such as diffusion paths and concentration profiles in the Ni-Ti-V ternary system can be reasonably described by the obtained atomic mobilities. This work contributes to the establishment of nickel-based kinetic database.

Keywords atomic mobility · DICTRA · diffusion couples · interdiffusion coefficients · Ni-Ti-V alloys

1 Introduction

Nickel-based superalloys have high strength, excellent high-temperature fatigue resistance, good gas corrosion resistance and oxidation resistance.^[1–3] The excellent properties of nickel-based superalloys are related to their precipitation strengthening mechanism.^[4] The L1₂-ordered γ' phase is uniformly precipitated in the fcc- γ matrix phase after heat treatment,^[5,6] which enhances the high-temperature strength and creep resistance of nickel-based superalloys. Alloying with titanium and vanadium can promote the formation of γ' -phase^[7] in nickel-based superalloys. In addition, adding titanium to nickel-based superalloys can reduce the specific weight and improve its high-temperature corrosion resistance, fatigue resistance and strength,^[8,9] while the addition of vanadium can improve the high-temperature strength and mechanical properties.^[10,11] The study of kinetic behavior of the Ni-Ti-V ternary system is essential for understanding how temperature, time and alloy composition affect the microstructure and properties of superalloys.

Over the past few decades, CALPHAD (calculation of phase diagrams) has been one of the major success stories in the development of materials science, combining fewer experimental measurements and thermodynamic calculation data to produce a candidate alloy with the required composition and phase constitution for a particular application. The extensive application of the “CALPHAD” method in the field of alloy design and process improvement has replaced the “trial and error” method, which has changed the situation of low efficiency and high cost in alloy design.^[12] DICTRA, a computational software package designed within the CALPHAD framework, can simulate diffusion-controlled processes with the help of

✉ Y. Lu
luyong@xmu.edu.cn

✉ X. J. Liu
lxj@xmu.edu.cn

¹ College of Materials and Fujian Key Laboratory of Surface and Interface Engineering for High Performance Materials, Xiamen University, Xiamen, People's Republic of China

² Institute of Materials Genome and Big Data, Harbin Institute of Technology, Shenzhen, People's Republic of China

thermodynamic and kinetic databases, and thus is widely used in the study of different types of materials.^[13]

Up to now, many experimental studies on the atomic mobilities of binary subsystems have been established, including the atomic mobilities of fcc Ni-Ti and fcc Ni-V binary of the Ni-Ti-V system reported by Liu et al.^[14] Meanwhile, many ternary interdiffusion systems have also been studied, such as Ni-Cu-Ti,^[15,16] Ni-Nb-Ti,^[17] Ni-Mo-Ti,^[18] Ni-Fe-V.^[19] However, the kinetic assessment of Ni-Ti-V ternary system has not been carried out yet. The main objectives of this study are: (1) to determine the interdiffusion coefficients of fcc Ni-Ti-V ternary system annealed at 1373 and 1473 K for 72 and 48 h; (2) accurately assess the atomic mobility parameters of fcc Ni-Ti-V ternary system by DICTRA software package based on literature and experimental results; (3) to verify the reliability of the atomic mobility parameters obtained in this study by comprehensive comparison between the experimental data and the corresponding diffusion characteristics predicted by the model.

2 Experimental Procedure

Ni (purity: 99.9 wt.%), Ti (purity: 99.9 wt.%) and V (purity: 99.9 wt.%) were used as raw materials for the preparation of ternary alloys. In Fig. 1, the 1373 and 1473 K isothermal sections of the Ni-Ti-V ternary system on the nickel-rich side were calculated based on the thermodynamic data reported by Zou et al.,^[20] and the dashed dot lines in the figure represent the ten sets of diffusion couples. The specific components of the ten groups of

diffusion couples are shown in Table 1, and the preparation steps were as follows:

Firstly, the alloys designed in this study were melted into metal ingots with a mass of 30 g by arc melting under high-purity argon atmosphere. Metal ingots were repeatedly turned and melted at least five times to improve the homogeneity. The metal ingots were cut into cuboids with size of $4 \times 4 \times 7 \text{ mm}^3$ by wire-electrode discharging machine. The cuboid samples were polished using coarse sandpaper to remove oil stains and oxides from the surface. Secondly, the alloy samples were vacuum-packed with quartz tubes, and the solid-solution treatment was carried out at 1473 K for 5 days to make the composition of the alloys more homogeneous and promote the growth of grains to reduce the influence of grain boundaries on the diffusion process. All surfaces of the alloy samples were polished again, and for better bonding, one of the surfaces with the size of $4 \times 7 \text{ mm}^2$ was polished to the mirror surface using $0.05 \mu\text{m}$ alumina. Subsequently, the diffusion couples were tightly bound by Mo wires, and then vacuum encapsulated by quartz tubes. The diffusion couples were annealed at 1373 and 1473 K for 259,200 (72) and 172,800 s (48 h), respectively, and then quenched with ice water to retain their single fcc-phase state. The diffusion couples were cut perpendicular to the diffusion interface using wire-electrode discharging machine, and the diffusion interface was polished to the mirror surface using $0.05 \mu\text{m}$ alumina. After standard metallographic preparation, these annealed diffusion couples, as shown in Table 1, were tested by EPMA (electron probe micro analysis, JXA-8100, JEOL, Japan, the accelerating voltage and probe

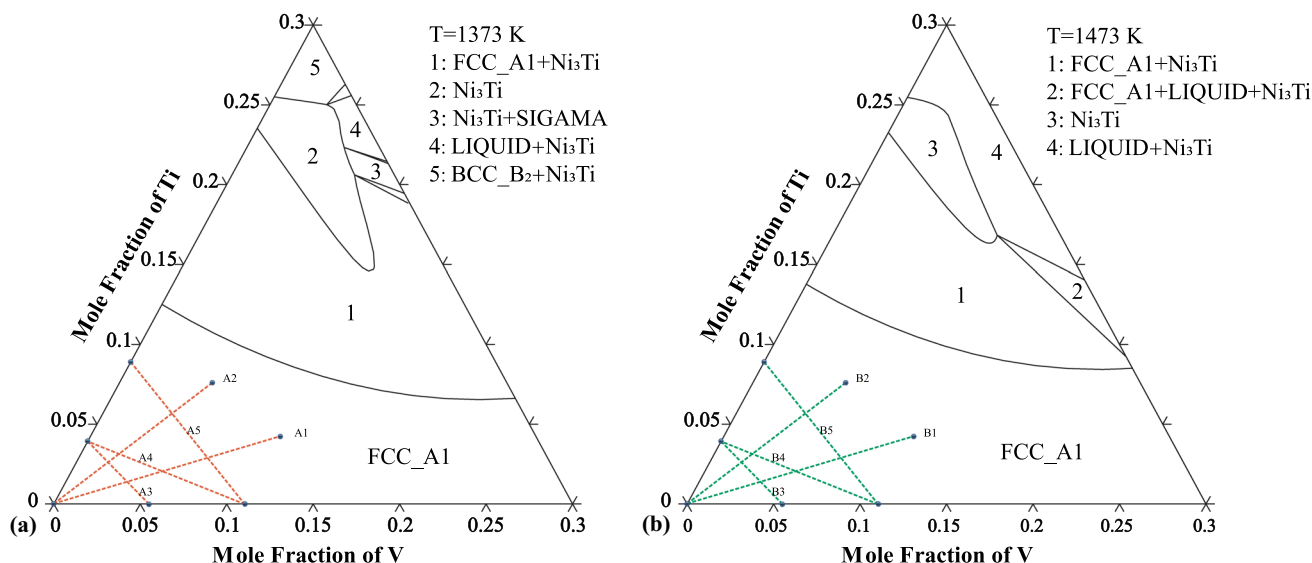


Fig. 1 Calculated isothermal sections in Ni-rich corner of Ni-Ti-V system using the thermodynamic parameters of Zou et al.^[20] (a) at 1373 K (b) 1473 K

Table 1 List of nominal compositions for the diffusion couples in this work.

Couple name	Composition (at. %)	Temperature(K)	Diffusion time (s)
A1	Ni/Ni-4.30Ti-10.50 V	1373	259200
A2	Ni/Ni-7.40Ti-5.20 V	1373	259200
A3	Ni-4.35Ti/Ni-5.30 V	1373	259200
A4	Ni-4.35Ti/Ni-10.60 V	1373	259200
A5	Ni-8.50Ti/Ni-10.60 V	1373	259200
B1	Ni/Ni-4.30Ti-10.50 V	1473	172800
B2	Ni/Ni-7.40Ti-5.20 V	1473	172800
B3	Ni-4.35Ti/Ni-5.30 V	1473	172800
B4	Ni-4.35Ti/Ni-10.60 V	1473	172800
B5	Ni-8.50Ti/Ni-10.60 V	1473	172800

current were 20 kV and 1.0×10^{-8} A, respectively) to measure the local concentration profiles.

3 Modeling of Atomic Mobility

3.1 Determination of Interdiffusion Coefficients

According to Kirkaldy,^[21] Fick's second law of diffusion for a component i of concentration C_i in a ternary system can be given as:

$$\frac{\partial C_i}{\partial t} = \sum_{j=1}^2 \frac{\partial}{\partial x} \left(\tilde{D}_{ij}^3 \frac{\partial C_j}{\partial x} \right) \quad \text{for } i, j = 1, 2 \quad (\text{Eq 1})$$

where C_i is concentration of element i , x is the distance, t represents time, and \tilde{D}_{ij}^3 is the interdiffusion coefficient where 3 represents the solvent. \tilde{D}_{ij}^3 has different meanings when the values of i and j are the same or different. The main interdiffusion coefficients, \tilde{D}_{11}^3 and \tilde{D}_{22}^3 , represent the influence of the concentration gradients of elements 1 and 2 on their own fluxes. While \tilde{D}_{12}^3 and \tilde{D}_{21}^3 are called cross interdiffusion coefficients which represent the influences of the concentration gradients of element 2 and element 1 on the fluxes of each other. Under the usual initial and boundary conditions prevalent for semi-infinite diffusion couples, we have

$$\begin{aligned} C_i(-x, 0) &= C_i(-\infty, t) = C_i^- \\ C_i(x, 0) &= C_i(+\infty, t) = C_i^+ \quad \text{for } i = 1, 2 \end{aligned} \quad (\text{Eq 2})$$

Then the solutions of Eq 1 are:

$$\int_{C_i^-}^{C_i} x dC_i = -2t \sum_{j=1}^2 \tilde{D}_{ij}^3 \frac{dC_j}{dx} \quad (\text{Eq 3})$$

Whittle and Green^[22] introduce the normalized concentration parameter $Y_i = (C_i - C_i^-)/(C_i^+ - C_i^-)$ to avoid the calculating of Matano interface, so the Eq 3 can be transformed into the following equation^[23]:

$$\begin{aligned} \frac{1}{2t} \frac{dx}{dY_1} \left[(1 - Y_1) \int_{-\infty}^x Y_1 \cdot dx + Y_1 \int_x^{+\infty} (1 - Y_1) \cdot dx \right] \\ = \tilde{D}_{11}^3 + \tilde{D}_{12}^3 \frac{C_2^+ - C_2^-}{C_1^+ - C_1^-} \cdot \frac{dY_2}{dY_1} \end{aligned} \quad (\text{Eq 4})$$

$$\begin{aligned} \frac{1}{2t} \frac{dx}{dY_2} \left[(1 - Y_2) \int_{-\infty}^x Y_2 \cdot dx + Y_2 \int_x^{+\infty} (1 - Y_2) \cdot dx \right] \\ = \tilde{D}_{22}^3 + \tilde{D}_{21}^3 \frac{C_1^+ - C_1^-}{C_2^+ - C_2^-} \cdot \frac{dY_1}{dY_2} \end{aligned} \quad (\text{Eq 5})$$

To solve for the four diffusion coefficients in Eq 4 and 5, two pairs of diffusion couple whose diffusion paths intersect at a common concentration are required.

3.2 Modeling of Atomic Mobility

According to the theory of absolute-reaction rate,^[24,25] the atomic mobility of a certain component is taken as the optimization variable, and the atomic mobility M of this component is defined as a function of pressure, temperature and composition. The atomic mobility of element B, M_B , can be divided into frequency factor M_B^0 and activation enthalpy Q_B ^[26,27], M_B can be described as

$$M_B = M_B^0 \exp\left(-\frac{Q_B}{RT}\right) \frac{1}{RT} \text{mg}\Gamma \quad (\text{Eq 6})$$

where T is the absolute temperature and R is the gas constant, $\text{mg}\Gamma$ is a magnetic-related transformation factor, which is taking into account the effect of the ferromagnetic transition^[28]. It has been suggested^[29] that the logarithm of the frequency factor ($\ln M_B^0$) should be expanded rather than the value itself, thus the mobility M_B is expressed as

$$M_B = \exp\left(\frac{RT \ln M_B^0}{RT}\right) \exp\left(-\frac{Q_B}{RT}\right) \frac{1}{RT} \text{mg}\Gamma \quad (\text{Eq 7})$$

For the high-temperature fcc phase in Ni-Ti-V ternary system, the contribution of ferromagnetism to diffusion is negligible, $\text{mg}\Gamma = 1$, then M_B^0 and Q_B can be merged into one parameter: $\Phi_B = RT \ln M_B^0 - Q_B$, Φ_B can be

represented by the Redlich–Kister polynomial^[30] for binary terms and a power series expansion for ternary terms^[31]:

$$\Phi_B = \sum_i x_i \Phi_B^i + \sum_i \sum_{j>i} x_i x_j \left[\sum_{r=0}^m r \Phi_B^{i,j} (x_i - x_j)^r \right] + \sum_i \sum_{j>i} \sum_{k>j} x_i x_j x_k \left[v_{ijk}^s \Phi_B^{i,j,k} \right] \quad (s = i, j \text{ or } k) \tag{Eq 8}$$

where x_i, x_j and x_k are mole fractions of elements i, j and k , Φ_B^i is the value of Φ_B for pure i and thus represents one of the endpoint values in the composition space. $r\Phi_B^{i,j}$ is the binary interaction parameter, v_{ijk}^s are the ternary interaction parameters. Any Φ parameter can be described by a polynomial of temperature and pressure. The parameter v_{ijk}^s , it can be expressed as:

$$v_{ijk}^s = x_s + \frac{1 - x_i - x_j - x_k}{3} \tag{Eq 9}$$

where x_s is the mole fraction of element s .

The diffusion mobility can be related to the diffusion coefficient, assuming a mono-vacancy mechanism coupled neglecting correlation factors, and the tracer diffusivity D_B^* is directly related to the mobility M_B by means of the Einstein relation^[32]

$$D_B^* = RTM_B \tag{Eq 10}$$

The interdiffusion coefficients with n as the dependent species are correlated to the atomic mobility by

$$\tilde{D}_{kj}^n = \sum_i (\delta_{ik} - x_k) \cdot x_i \cdot M_i \cdot \left(\frac{\partial \mu_i}{\partial x_j} - \frac{\partial \mu_i}{\partial x_n} \right) \tag{Eq 11}$$

where δ_{ik} is the Kronecker delta, if $i = k, \delta_{ik} = 1$; if $i \neq k, \delta_{ik} = 0$. The x_i, μ_i and M_i are the mole fraction, chemical potential, and mobility of element i , respectively.

4 Results and Discussion

4.1 Interdiffusion Coefficients

To solve the interdiffusion coefficient at the intersection of diffusion paths, it is necessary to obtain the fitting equations for the concentration-distance curves of each diffusion couple. The square symbols in Fig. 2 are the data obtained after smoothing the concentration-distance curve of diffusion couple B4(Ni-4.35Ti/Ni-10.6 V) by MATLAB software, and the solid line is the fitting curves obtained by Gaussian fitting of the smoothed data. Figure 3 shows the distribution of interdiffusion flux calculated based on the Gaussian fitting equation of the concentration-distance

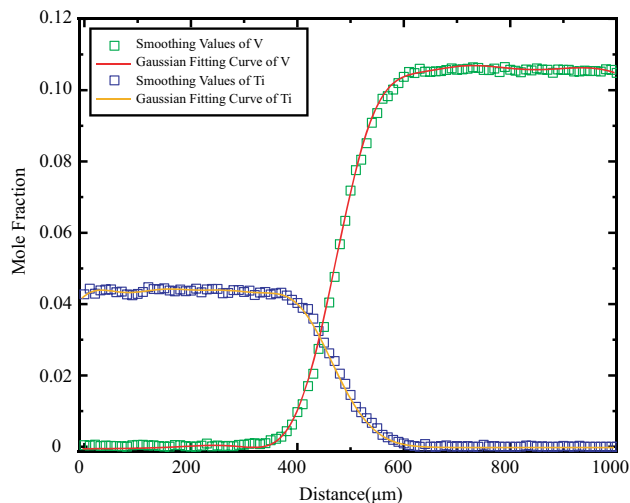


Fig. 2 The smoothed values and Gaussian fitting curves of the concentration-distance curves of diffusion couple B4(Ni-4.35Ti/Ni-10.6 V)

curve of each element in the diffusion couple. After analysis, it is found that the interdiffusion flux is distributed symmetrically near the diffusion interface and tends to smoothly approach zero at both ends. Based on the diffusion experiment in the Gibbs triangle of Ni-rich Ni-Ti-V system and Gaussian fitting equations, four interdiffusion coefficients $\tilde{D}_{TiTi}^{Ni}, \tilde{D}_{TiV}^{Ni}, \tilde{D}_{VV}^{Ni}, \tilde{D}_{VTi}^{Ni}$ at the intersection composition of the diffusion paths were determined based on the Whittle and Green method, using Eq 4 and 5. The experimentally measured main interdiffusion coefficients ($\tilde{D}_{TiTi}^{Ni}, \tilde{D}_{VV}^{Ni}$) and the corresponding cross interdiffusion coefficients ($\tilde{D}_{TiV}^{Ni}, \tilde{D}_{VTi}^{Ni}$) along with the DICTRA-extracted coefficients are listed in Table 2. It is obvious that the main interdiffusion coefficients \tilde{D}_{TiTi}^{Ni} and \tilde{D}_{VV}^{Ni} are larger than the absolute values of the cross interdiffusion coefficients \tilde{D}_{TiV}^{Ni} and \tilde{D}_{VTi}^{Ni} . Meanwhile, the values of \tilde{D}_{TiTi}^{Ni} are generally larger than those of \tilde{D}_{VV}^{Ni} , which means that the diffusion rates of Ti is higher than that of V in the Ni-Ti-V ternary system. The values of \tilde{D}_{TiV}^{Ni} and \tilde{D}_{VTi}^{Ni} are positive and have the same order of magnitude as those of \tilde{D}_{TiTi}^{Ni} and \tilde{D}_{VV}^{Ni} . This indicates that Ti and V have a certain degree of influence on the diffusion process of each other and shows that Ti diffuses toward the direction of low V concentration, and V diffuses toward the direction of low Ti concentration. Furthermore, all currently obtained interdiffusion coefficients need to strictly satisfy the following constraints to ensure the stability of solid solutions,^[33]

$$\tilde{D}_{TiTi}^{Ni} + \tilde{D}_{VV}^{Ni} > 0 \tag{Eq 12}$$

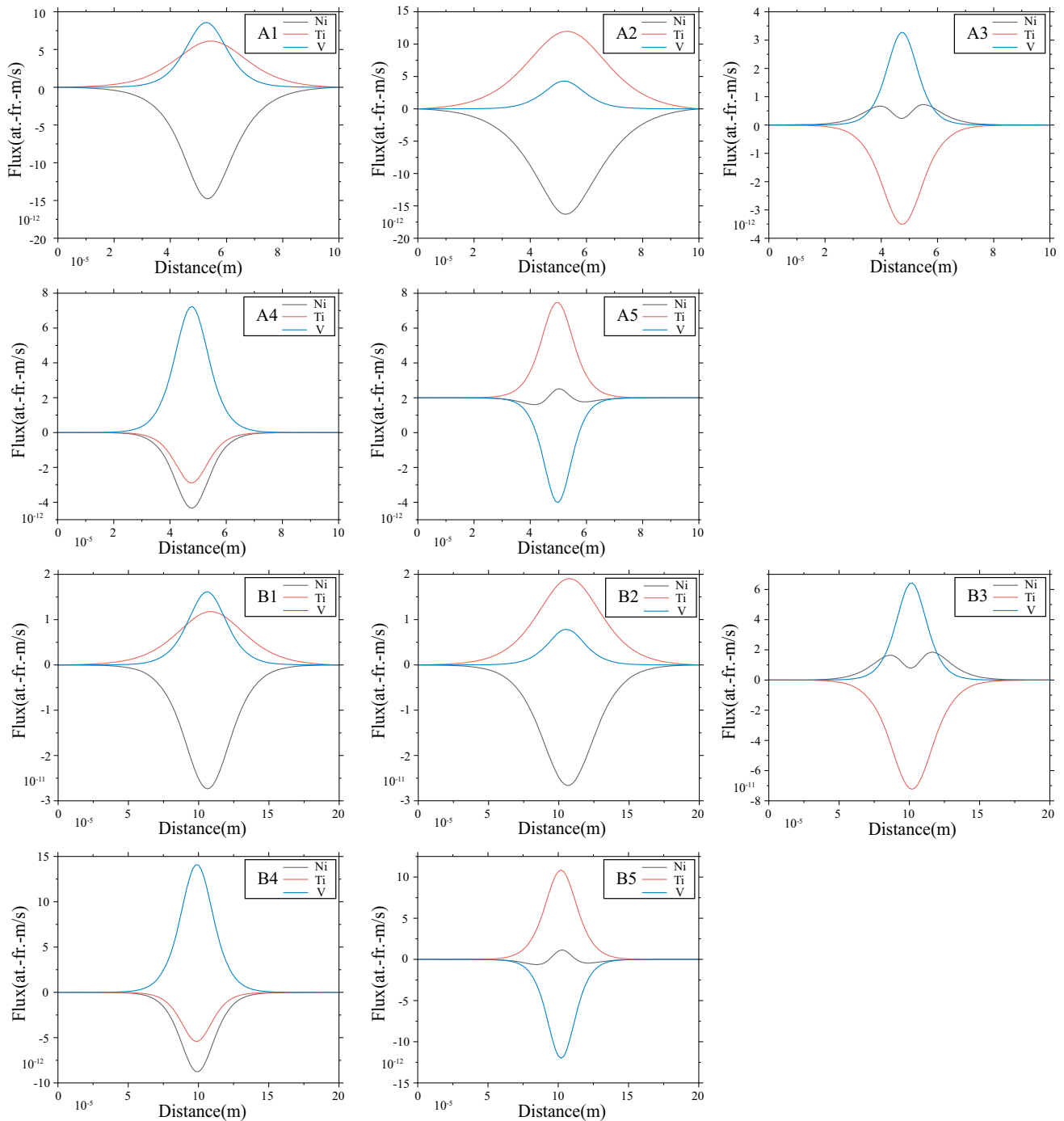


Fig. 3 Interdiffusion flux distribution calculated based on the Gaussian fitting equation of the concentration-distance curves of diffusion couples (A1–A5 and B1–B5).

$$\tilde{D}_{TiTi}^{Ni} \cdot \tilde{D}_{Vv}^{Ni} - \tilde{D}_{TiV}^{Ni} \cdot \tilde{D}_{Vti}^{Ni} \geq 0 \quad (\text{Eq 13})$$

$$(\tilde{D}_{TiTi}^{Ni} - \tilde{D}_{Vv}^{Ni})^2 + 4\tilde{D}_{TiV}^{Ni} \cdot \tilde{D}_{Vti}^{Ni} \geq 0 \quad (\text{Eq 14})$$

Substituting the presently obtained interdiffusion coefficients into Eq 12–14 and one finds that they all strictly satisfy these constraints. Therefore, it can be proved that

the interdiffusion coefficients obtained in this study are reliable.

4.2 Assessment of Atomic Mobility

Since the assessment of diffusivities is based on the thermodynamic description, reasonable thermodynamic

Table 2 Experimental interdiffusion coefficients and DICTRA-extracted diffusivities in fcc Ni-Ti-V alloys

Intersection diffusion paths	Temperature, K	Composition, at. %		Interdiffusion coefficients, $10^{-15} \text{ m}^2 \text{ s}^{-1}$				DICTRA-extracted diffusivities, $10^{-15} \text{ m}^2 \text{ s}^{-1}$			
		Ti	V	\tilde{D}_{TTi}^{Ni}	\tilde{D}_{TiV}^{Ni}	\tilde{D}_{VV}^{Ni}	\tilde{D}_{VTi}^{Ni}	\tilde{D}_{TTi}^{Ni}	\tilde{D}_{TiV}^{Ni}	\tilde{D}_{VV}^{Ni}	\tilde{D}_{VTi}^{Ni}
A1–A3	1373	1.49	3.58	16.7	4.03	9.64	5.74	15.2	3.14	8.26	4.22
A1–A4	1373	1.94	5.82	15.6	3.53	9.45	5.51	13.9	3.14	8.28	5.47
A1–A5	1373	2.54	7.89	13.0	4.17	9.14	6.63	13.4	3.28	8.06	6.04
A2–A3	1373	2.82	1.70	24.2	9.84	8.23	2.07	23.1	7.01	7.17	2.19
A2–A4	1373	3.35	2.54	23.3	7.97	8.05	2.01	23.2	7.45	7.18	2.97
A2–A5	1373	4.96	4.46	20.4	9.54	5.83	1.04	24.2	8.76	7.04	4.32
B1–B3	1473	1.54	3.46	93.4	15.9	48.9	20.4	73.2	14.5	40.6	19.3
B1–B4	1473	1.92	5.71	84.2	15.0	46.3	30.5	62.5	13.2	40.8	25.7
B1–B5	1473	2.41	7.91	74.3	20.4	47.9	30.7	55.5	12.4	40.0	28.9
B2–B3	1473	2.75	1.75	106	22.4	42.5	10.5	110	31.2	37.1	10.7
B2–B4	1473	3.28	2.78	90.7	23.0	38.2	18.4	105	31.7	37.4	15.2
B2–B5	1473	4.91	4.34	76.9	24.4	33.3	11.6	108	36.8	36.0	19.4

parameters are necessary to obtain more accurate atomic mobility parameters. The thermodynamic description of the Ni-Ti-V ternary system used in this work is directly taken from the work of Zou et al.^[20] The calculated partial isothermal sections of the Ni-Ti-V ternary system at 1373 and 1473 K are shown in Fig. 1(a) and (b). The atomic mobilities for the self-diffusion of Ni, Ti and V are taken from Zhang et al.^[34] Zhou et al.^[35] and Liu et al.,^[14] respectively. And the atomic mobility parameters for the Ni-Ti, Ni-V binary systems are also obtained from the report of Liu et al.^[14] Since fcc Ti and V are metastable phases, the impurity diffusion coefficients in hypothetical fcc Ti and V cannot be determined through experiment. For simplicity, the impurity diffusion coefficients of V in fcc-Ti are assumed to be equal to the self-diffusion coefficient of fcc-Ti, and the impurity diffusion coefficient of Ti in fcc-V is assumed to be equal to the self-diffusion coefficient of V in fcc-V in the present work. The atomic mobilities from other literature cited in this study are listed in Table 3. The atomic mobilities of the fcc Ni-Ti-V ternary system were evaluated using the PARROT module of DICTRA software according to the available binary atomic mobilities in Table 3 and the experimental interdiffusion coefficients in Table 2, and the results are shown in Table 3. Then, the interdiffusion coefficients were evaluated using the DICTRA software combined with the obtained atomic mobility parameters, and the detailed values are listed in Table 2.

In Fig. 4, the main diffusion coefficients corresponding to the intersections of the diffusion paths are listed. The solid squares in the figure represent the intersections, the calculated values, and experimental values of the main

Table 3 Assessed mobility parameters for fcc Ni-Ti-V alloys.

Mobility	Parameters, J/mol	References
Ni	$\Phi_{Ni}^{Ni} = -271377.6 - 81.79 * T$	[29]
	$\Phi_{Ni}^{Ti} = -132849.8 - 81.40 * T$	[14]
	$\Phi_{Ni}^{Ni,Ti} = 351220.4$	[14]
	$\Phi_{Ni}^V = -197683.6 - 79.32 * T$	[14]
	${}^0\Phi_{Ni}^{Ni,V} = -135325.8$	[14]
	${}^1\Phi_{Ni}^{Ni,V} = 44311.8$	[14]
	$\Phi_{Ni}^{Ti,V} = -250573.19 + 134.03 * T$	This work
Ti	$\Phi_{Ti}^{Ti} = -132849.8 - 81.40 * T$	[30]
	$\Phi_{Ti}^{Ni} = -276771.3 - 63.82 * T$	[14]
	$\Phi_{Ti}^V = -197683.64 - 79.35 * T$	This work
	$\Phi_{Ti}^{Ti,Ni} = -176117.8$	[14]
	$\Phi_{Ti}^{Ni,V} = 295958 - 345.61 * T$	This work
V	$\Phi_V^V = -197683.64 - 79.35 * T$	[14]
	$\Phi_V^{Ni} = -265821.1 - 76.39 * T$	[14]
	$\Phi_V^{Ti} = -132849.8 - 81.40 * T$	This work
	${}^0\Phi_V^{V,Ni} = -82265$	[14]
	${}^1\Phi_V^{V,Ni} = -71078.1$	[14]
	$\Phi_V^{Ni,Ti} = -842506.98 + 427.26 * T$	This work

interdiffusion coefficients are given inside brackets and outside brackets, respectively. In Fig. 5, the experimentally measured main interdiffusion coefficients are compared with the calculated main interdiffusion coefficients. The

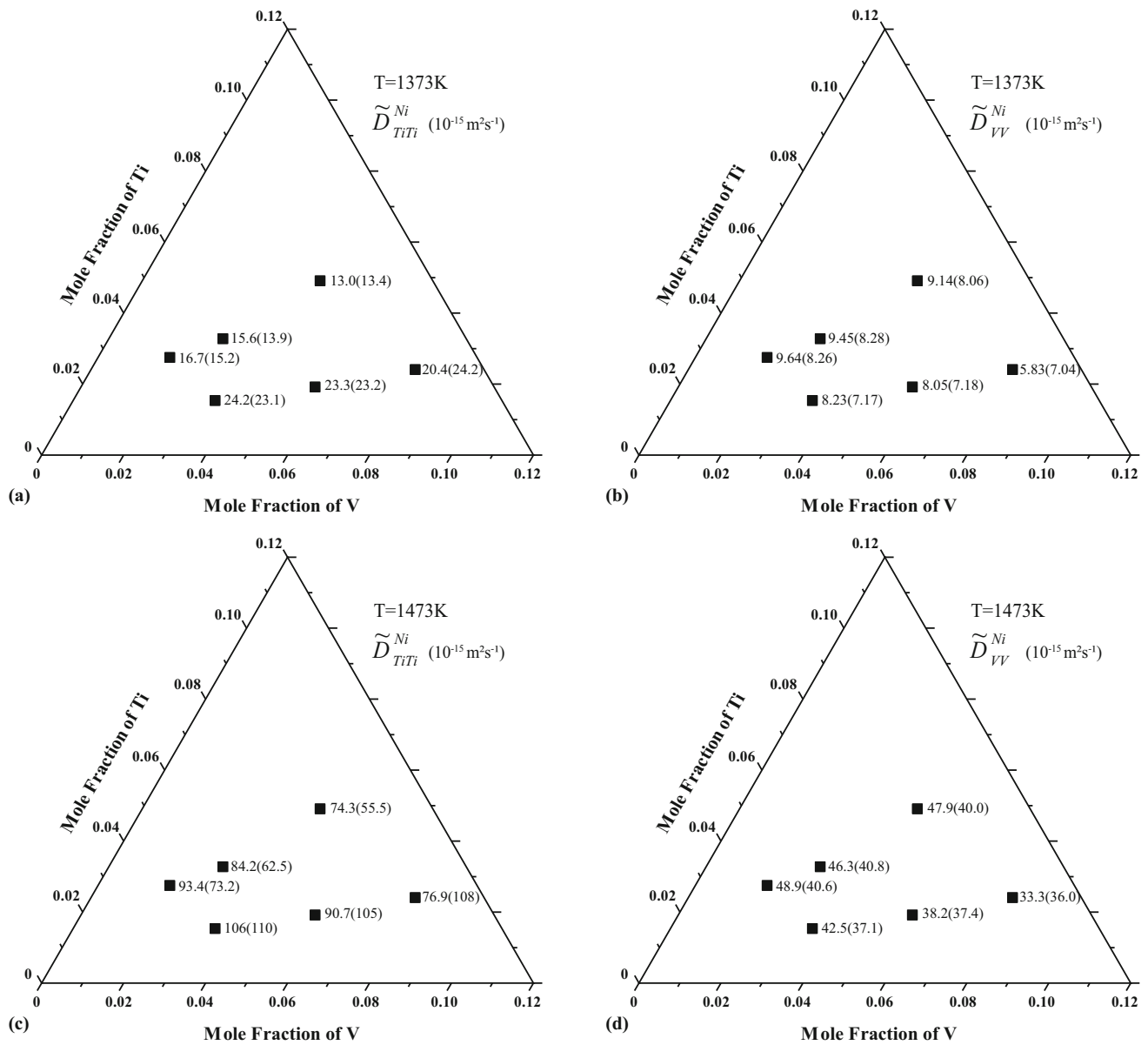


Fig. 4 Comparison between the calculated main interdiffusion coefficients (numbers in brackets) and the experimental measurements

points around the diagonal line are the logarithms of the main interdiffusion coefficients obtained from this work. The dashed lines with a factor of 2 or 0.5 from the diagonal line are shown as well. Such a factor is a generally accepted experimental error for the measurement of diffusivities.^[36] As can be seen, the main interdiffusion coefficients are all within the dashed range, and there is a good match between the experimental results and calculated data. After comprehensive analysis of the cross interdiffusion coefficients in Table 2, it can be found that the calculated values are all within the range of 0.5–2 times of the experimental values, which shows that there is a good consistency between the calculated values and the

experimental values. This also further verifies the rationality of the atomic mobilities obtained in this study.

4.3 Validation of the Present Atomic Mobility

Simple comparison between the calculated interdiffusion coefficients and the experimental ones is far from sufficient to verify the reliability of the estimated diffusional mobilities. To further evaluate the reliability of the diffusion mobility database, the diffusion behaviors such as the concentration-distance profiles and the diffusion paths of each diffusion couple were compared with the experimental data from this work. Figure 6 presents the

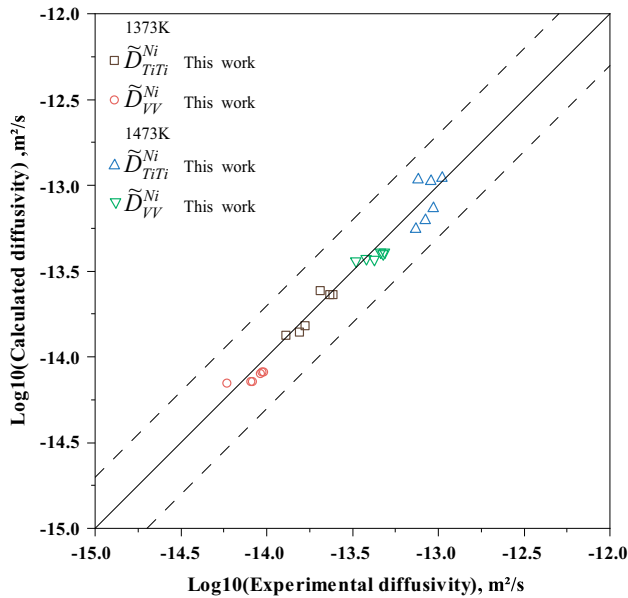


Fig. 5 Comparison between the calculated major interdiffusion coefficients of the fcc Ni-Ti-V system and the experimental values at 1373 and 1473 K. Dashed lines refer to the diffusion coefficients with a factor of 2 or 0.5 from the model-predicted ones

comparisons between the calculated concentration-distance profiles for Ti and V in the diffusion couples (A1, A2, A3, A4, A5) annealed at 1373 K for 259,200 s and the experimentally measured data. Figure 7 presents the comparisons between the calculated concentration-distance profiles for Ti and V in the diffusion couples (B1, B2, B3, B4, B5) annealed at 1473 K for 172,800 s and the experimentally measured data. It is evident that the calculated curves fit the experimental data well, which confirms the reliability of the mobility parameters obtained in this work. It can be seen from Fig. 6 and 7 that the diffusion distance of Ti is longer than that of V, indicating that the diffusion speed of Ti is faster. At the same time, it can also be found that because of the cross interdiffusion coefficients, the diffusion distances of Ti in the diffusion couples A1, A2, B1 and B2 are larger than those in the diffusion couples A3, A4, A5, B3, B4 and B5.

For the diffusion path of a diffusion couple, the eccentricity will increase as the difference between the two main diffusion coefficients increases. If the two main diffusion coefficients are equal, the diffusion path will exist as a straight line on the isothermal section of the Ni-Ti-V ternary phase diagram.^[37] When the diffusion path is S-shaped, it is due to the difference in diffusion coefficients

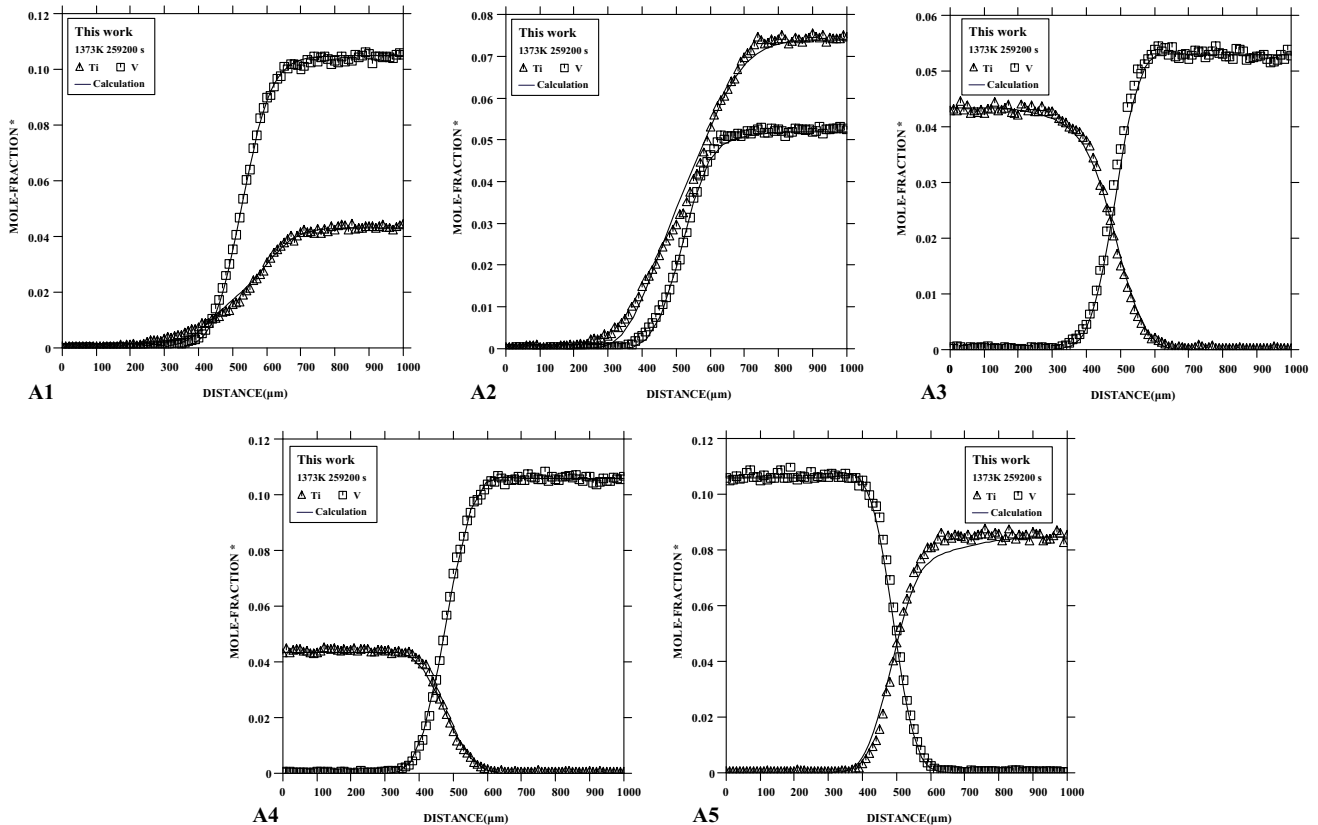


Fig. 6 Comparison between the experimental and DICTRA-simulated concentration profiles for the diffusion couples annealed at 1373 K for 259,200 s. A1: Ni/Ni-4.3Ti-10.5 V, A2: Ni/Ni-7.4Ti-5.2 V, A3: Ni-4.35Ti/Ni-5.3 V, A4: Ni-4.35Ti/Ni-10.6 V, A5: Ni-8.5Ti/Ni-10.6 V

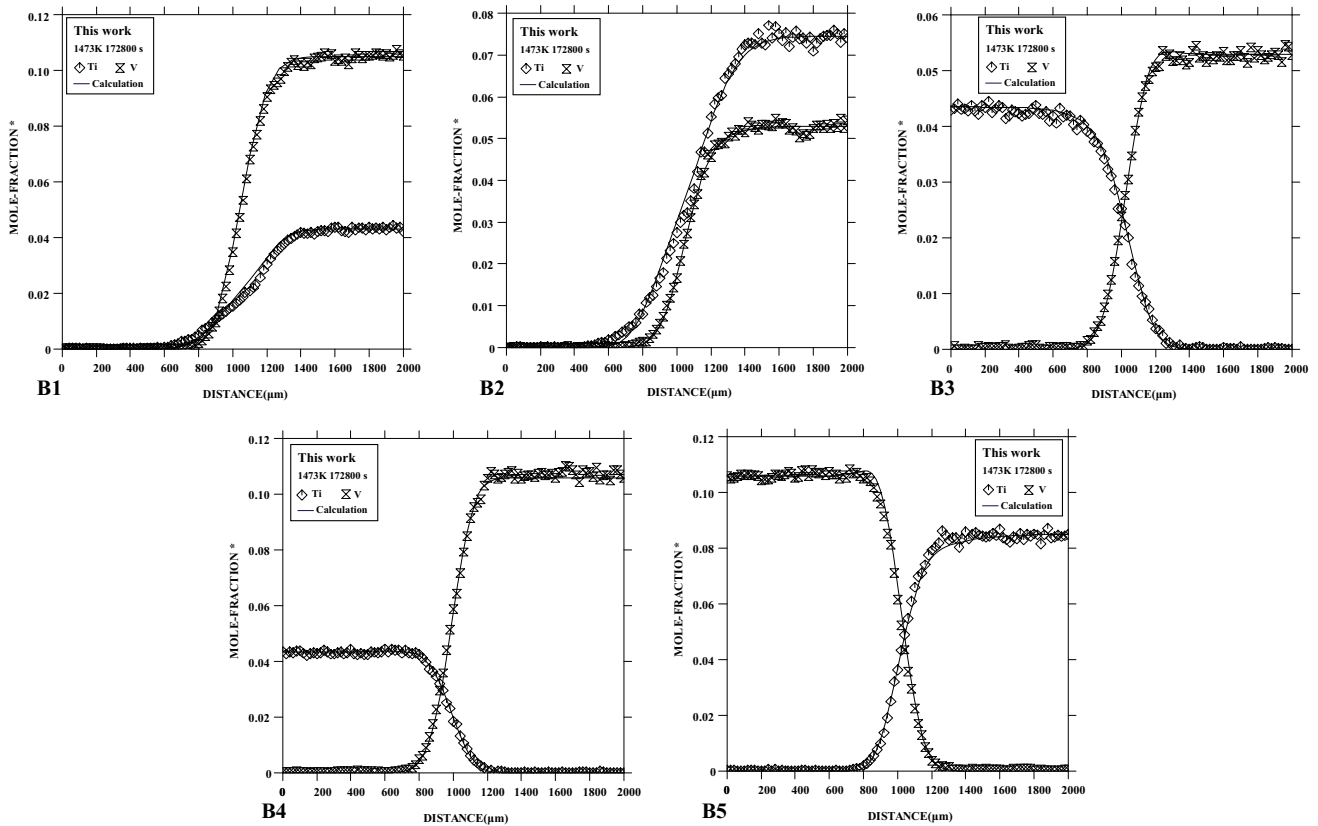


Fig. 7 Comparison between the experimental and DICTRA-simulated concentration profiles for the diffusion couples annealed at 1473 K for 172,800 s. B1: Ni/Ni-4.3Ti-10.5 V, B2: Ni/Ni-7.4Ti-5.2 V, B3: Ni-4.35Ti/Ni-5.3 V, B4: Ni-4.35Ti/Ni-10.6 V, B5: Ni-8.5Ti/Ni-10.6 V

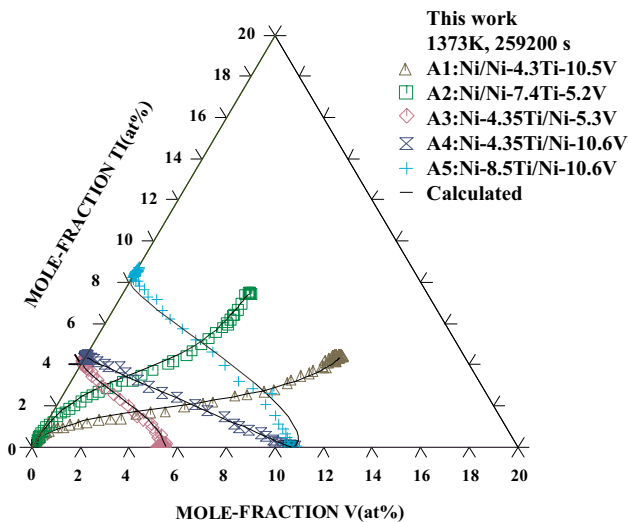


Fig. 8 Comparison between the experimental and DICTRA-simulated diffusion paths for various ternary Ni-Ti-V diffusion couples annealed at 1373 K for 259,200 s

and the mass balance of diffusing species in the solid-solid diffusion couple.^[21] Figure 8 and 9 show the calculated diffusion paths for various ternary diffusion couples (A1, A2, A3, A4, A5, B1, B2, B3, B4, B5) annealed at 1373 and

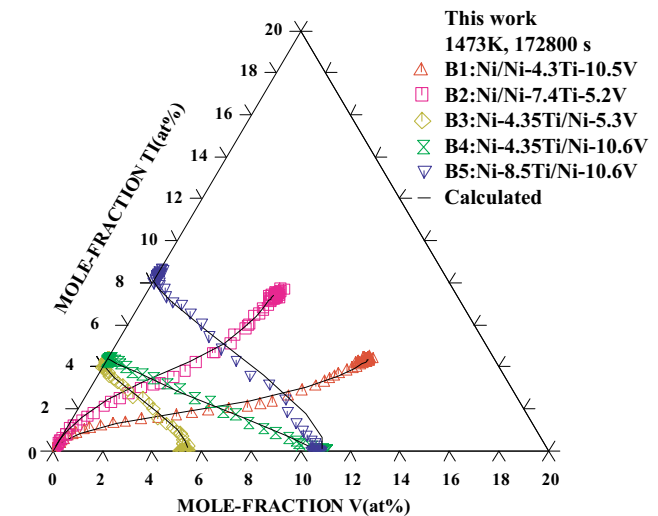


Fig. 9 Comparison between the experimental and DICTRA-simulated diffusion paths for various ternary Ni-Ti-V diffusion couples annealed at 1473 K for 172,800 s

1473 K for 259,200 and 172,800 s, respectively, compared with the corresponding experimental data. After analysis, it is found that the diffusion paths of diffusion couples A4 and B4 are straight lines, while the paths of other diffusion

couples are S-shaped. This is because cross interdiffusion coefficients is positive, and for the diffusion couples A4 and B4 (Ni-4.35Ti/Ni-10.6 V), the concentration gradient of Ti is small, while the concentration gradient of V is large. Therefore, the resistance of Ti to diffuse from Ni-4.35Ti alloy to Ni-10.6 V alloy is relatively large, which makes the diffusion of Ti in diffusion couples A4 and B4 more difficult than in other diffusion couples, making the diffusion distance of Ti like V, so the diffusion paths of diffusion couples A4 and B4 is a straight line. As can be seen from the figures, the calculated results agree well with the experimental values, which also proves the rationality and validity of the mobility parameters obtained in this study.

5 Conclusions

In this work, ten diffusion couples for fcc Ni-Ti-V alloys were annealed at 1373 and 1473 K for 259,200 and 172,800 s, respectively. The interdiffusion coefficients for fcc Ni-Ti-V ternary system were determined by means of EPMA and Whittle and Green method. By using DICTRA software package, the atomic mobilities of the Ni-Ti-V ternary alloys were assessed based on the available thermodynamic data, the atomic mobilities of binary systems reported in the literature and the experimental data obtained from the present work. The results show that titanium diffuses faster than vanadium in the nickel-rich alloys. The reliability of the experimental interdiffusivities is validated via thermodynamic constraints. Meanwhile, in the comprehensive comparison, it was found that the calculated diffusion coefficients were in good agreement with the experimentally measured diffusion coefficients. Diffusion phenomena such as concentration-distance profiles and diffusion paths can be reasonably described. The atomic mobility parameters obtained in this work contributes to the establishment of nickel-based kinetic database and are valuable for nickel-based superalloy design.

Acknowledgments This work was supported by the National Natural Science Foundation of China (Grant No. 51831007), the Shenzhen Science and Technology Program (Grant No. SGD20210823104002016) and the Guangdong Basic and Applied Basic Research Foundation (No. 2021B1515120071).

Reference

1. T. Osada, N. Nagashima, Y. Gu, Y. Yuan, T. Yokokawa, and H. Harada, Factors Contributing to the Strength of a Polycrystalline Nickel-Cobalt Base Superalloy, *Scripta Mater.*, 2011, **64**(9), p 892–895.
2. D. Li, Q. Guo, S. Guo, H. Peng, and Z. Wu, The Microstructure Evolution and Nucleation Mechanisms of Dynamic Recrystallization in Hot-Deformed Inconel 625 Superalloy, *Mater Design.*, 2011, **32**(2), p 696–705.
3. D.M. Collins, and H.J. Stone, A Modelling Approach to Yield Strength Optimisation in a Nickel-Base Superalloy, *Int. J. Plast.*, 2014, **54**, p 96–112.
4. R.W. Kozar, A. Suzuki, W.W. Milligan, J.J. Schirra, M.F. Savage, and T.M. Pollock, Strengthening Mechanisms in Polycrystalline Multimodal Nickel-Base Superalloys, *Metall. Mater. Trans. A*, 2009, **40**(7), p 1588–1603.
5. W. Chen, W. Xing, H. Ma, X. Ding, X.-Q. Chen, D. Li, and Y. Li, Comprehensive First-Principles Study of Transition-Metal Substitution in the Γ Phase of Nickel-Based Superalloys, *Calphad*, 2018, **61**, p 41–49.
6. H. Bian, X. Xu, Y. Li, Y. Koizumi, Z. Wang, M. Chen, K. Yamanaka, and A. Chiba, Regulating the Coarsening of the γ' Phase in Superalloys, *NPG Asia Mater.*, 2015, **7**(8), p 212.
7. A. Bauer, S. Neumeier, F. Pyczak, and M. Goeken, Microstructure and Creep Strength of Different γ/γ' -Strengthened Co-Base Superalloy Variants, *Scripta Mater.*, 2010, **63**(12), p 1197–1200.
8. Y.H. Tan, H.H. Xu, and Y. Du, Isothermal Section at 927 Degrees C of Cr-Ni-Ti System, *T. Nonferr. Metal. Soc.*, 2007, **17**(4), p 711–714.
9. J.W. Huang, Y. Wang, J.J. Wang, X.G. Lu, and L.J. Zhang, Thermodynamic Assessments of the Ni-Cr-Ti System and Atomic Mobility of Its Fcc Phase, *J. Phase Equilib. Diffus.*, 2018, **39**(5), p 597–609.
10. S. Wen, Y. Du, Y. Liu, C. Du, and M. Chu, Atomic Mobilities and Diffusivities in Fcc_A1 Ni-Cr-V System: Modeling and Application, *Calphad*, 2020, **70**, p 101808.
11. C.C. Zhao, S.Y. Yang, Y. Lu, Y.H. Guo, C.P. Wang, and X.J. Liu, Experimental Investigation and Thermodynamic Calculation of the Phase Equilibria in the Fe-Ni-V System, *Calphad*, 2014, **46**, p 80–86.
12. P.J. Spencer, A Brief History of Calphad, *Calphad*, 2008, **32**(1), p 1–8.
13. A. Borgenstam, A. Engstrom, L. Hoglund, and J. Agren, Dictra, a Tool for Simulation of Diffusional Transformations in Alloys, *J. Phase Equilib.*, 2000, **21**(3), p 269–280.
14. M. Liu, L. Zhang, W. Chen, J. Xin, Y. Du, and H. Xu, Diffusivities and Atomic Mobilities in Fcc_A1 Ni-X (X=Ge, Ti and V) Alloys, *Calphad*, 2013, **41**, p 108–118.
15. C.L. Li, S.M. Huang, and Y.J. Liu, Simulation of Atomic Mobilities, Interdiffusivities and Diffusional Evolution in Fcc Ni-Cu-Ti Alloys, *J. Alloys Compd.*, 2019, **780**, p 293–298.
16. Y.L. Liu, T.B. Fu, H.X. Liu, C.F. Du, Q.H. Min, S.Y. Wen, Y. Du, and Z.S. Zheng, Diffusivity and Atomic Mobility for Fcc Ni-Cu-Ti Alloy: Measurements and an Intelligent Modeling, *Calphad*, 2020, **70**, p 101780.
17. C.P. Wang, Y.J. Lin, Y. Lu, Z.B. Wei, Y.Q. Zhang, J.J. Han, and X.J. Liu, Interdiffusion and Atomic Mobilities in Ni-Rich Fcc Ni-Nb-Ti Alloys, *Rare Metal Mat. Eng.*, 2019, **48**(6), p 1803–1808.
18. C.P. Wang, W.H. Zhang, X. Yu, Y.R. Cui, L.K. Bao, D.X. Cheng, K.H. Zheng, Y. Lu, and X.J. Liu, Interdiffusion and Atomic Mobilities in Fcc Ni-Ti-Mo Alloys, *J. Phase Equilib. Diffus.*, 2022, **43**(3), p 345–354.
19. H.X. Liu, S.Y. Wen, Y.L. Liu, Y. Du, Q.H. Min, S.H. Liu, and P. Zhou, Diffusivity and Atomic Mobility in Fcc Ni-Fe-V System: Experiment and Modeling, *J. Phase Equilib. Diffus.*, 2020, **41**(4), p 550–566.
20. L. Zou, C.P. Guo, C.R. Li, and Z.M. Du, Experimental Investigation and Thermodynamic Modeling of the Ni-Ti-V System, *Calphad*, 2019, **64**, p 97–114.
21. S.J. Kirkaldy, Diffusion in Multicomponent Metallic Systems, *Can. J. Phys.*, 2011, **47**(4), p 435–440.

22. D.P. Whittle, and A. Green, The Measurement of Diffusion Coefficients in Ternary Systems, *Scr. Metall.*, 1974, **8**(7), p 883–884.
23. F. Sauer, and V. Freise, Diffusion in Binären Gemischen mit Volumenänderung, *Z. Elektro. Ber. BunsenGes. Phys. Chem.*, 1962, **66**(4), p 353–362.
24. J. Ågren, Numerical Treatment of Diffusional Reactions in Multicomponent Alloys, *J. Phys. Chem. Solids.*, 1982, **43**(4), p 385–391.
25. J. Ågren, Diffusion in Phases with Several Components and Sub-Lattices, *J. Phys. Chem. Solids.*, 1982, **43**(5), p 421–430.
26. J.O. Andersson, and J. Ågren, Models for Numerical Treatment of Multicomponent Diffusion in Simple Phases, *J. Appl. Phys.*, 1992, **72**(4), p 1350–1355.
27. J.J. Hoyt, The Continuum Theory of Nucleation in Multicomponent Systems, *Acta Metall. Mater.*, 1990, **38**(8), p 1405–1412.
28. B. Jönsson, Ferromagnetic Ordering and Diffusion of Carbon and Nitrogen in Bcc Cr-Fe-Ni Alloys, *Int. J. Mater. Res.*, 1994, **85**(7), p 498–501.
29. C.P. Wang, S.Y. Qin, Y. Lu, Y. Yu, J.J. Han, and X.J. Liu, Interdiffusion and Atomic Mobilities in Fcc Co-Cr-Mo Alloys, *J. Phase Equilib. Diffus.*, 2018, **39**(4), p 437–445.
30. O. Redlich, and A.T. Kister, Algebraic Representation of Thermodynamic Properties and the Classification of Solutions, *Ind. Eng. Chem.*, 1948, **40**(2), p 345–348.
31. M. Hillert, Empirical Methods of Predicting and Representing Thermodynamic Properties of Ternary Solution Phases, *Calphad*, 1980, **4**(1), p 1–12.
32. B. Jönsson, Assessment of the Mobility of Carbon in Fcc C-Cr-Fe-Ni Alloys, *Z. Metallkd.*, 1994, **85**(7), p 502–509.
33. J.S. Kirkaldy, D. Weichert, and Z.U. Haq, Diffusion in Multicomponent Metallic Systems. Vi. Some Thermodynamic Properties of the D Matrix and the Corresponding Solutions of the Diffusion Equations, *Can. J. Phys.*, 1963, **41**, p 2166–2173.
34. L. Zhang, Y. Du, Q. Chen, I. Steinbach, and B. Huang, Atomic Mobilities and Diffusivities in the Fcc, L12 and B2 Phases of the Ni-Al System, *Int. J. Mater. Res.*, 2010, **101**(12), p 1461–1475.
35. Z. Zhou, Y. Liu, G. Sheng, F. Lei, and Z. Kang, A Contribution to the Ni-Based Mobility Database: Fcc Ni-Fe-Ti Ternary Alloy, *Calphad*, 2015, **48**, p 151–156.
36. G. Shang, Y. Lu, J. Wang, and X.-G. Lu, Experimental and Computational Studies of Atomic Mobilities for Fcc Al-Co-Cr Alloys, *J. Phase Equilib. Diffus.*, 2022, **43**(4), p 471–482.
37. J.S. Kirkaldy, and L.C. Brown, Diffusion Behaviour in Ternary, Multiphase Systems, *Can. Metall. Q.*, 1963, **2**, p 89–115.

Publisher's Note Springer Nature remains neutral with regard to jurisdictional claims in published maps and institutional affiliations.

Springer Nature or its licensor (e.g. a society or other partner) holds exclusive rights to this article under a publishing agreement with the author(s) or other rightsholder(s); author self-archiving of the accepted manuscript version of this article is solely governed by the terms of such publishing agreement and applicable law.